Jurnal Teknik Informatika (JUTIF)
P-ISSN: 2723-3863
E-ISSN: 2723-3871
Vol. 6, No. 5, October 2025, Page. 3002-3017
https://jutif.if.unsoed.ac.id
DOI: https://doi.org/10.52436/1.jutif.2025.6.5.5106

Brain Tumor Auto Segmentation On 3D MRI Using Deep Neural Network

Melda Agarina[1], Muh Royan Fauzi Maulana*[2], Sutedi[3], Arman Suryadi Karim[4]

[1,2,3,4] Department of Computer Science, Informatics and Business Institute Darmajaya, Bandar Lampung, Lampung, Indonesia

Email: [2]royanfauzimaulana25@gmail.com

Received : Jun 30, 2025; Revised : Aug 11, 2025; Accepted : Aug 17, 2025; Published : Oct 16, 2025

Abstract

Accurate and automated segmentation of brain tumours from Magnetic Resonance Imaging (MRI) is crucial for clinical diagnosis and treatment planning, yet it remains a significant challenge due to tumour heterogeneity and data imbalance. This research investigation examines the effectiveness of a 3D UNet architecture for the segmentation of brain tumours utilizing MRI imaging modalities. The research employs the BRATS 2021 dataset, which consists of 675 MRI datasets across four distinct imaging modalities (FLAIR, T1-Weighted, T1-Contrast, and T2-Weighted) and encompasses four distinct segmentation label classes. The employed model integrated soft dice loss and dice coefficient as its loss functions, with the objective of achieving convergence despite the presence of imbalanced data. While constraints related to resources limited the training process, the model yielded promising outcomes, exhibiting high accuracy (99.43%) and specificity (99.5%), The model aids medical professionals in understanding tumor growth and enhances treatment planning via segmentation predictions in surgery. Nevertheless, the sensitivity, particularly concerning non-enhancing tumour classes, persists as a significant challenge, underscoring the necessity for future research to concentrate on data-centric methodologies and enhanced pre-processing techniques to improve model efficacy in critical medical applications such as the segmentation of brain tumours.

Keywords : *Brain Tumor, CNN, DNN, Segmentation, 3D UNet*

1. INTRODUCTION

The development of information technology, particularly in the field of machine learning, has begun to be implemented in a number of other industries, including the health sector [1]. Machine learning is a subfield of artificial intelligence that employs algorithms to identify patterns in data and predict future outcomes [2], [3]. These predictions are based on the assumption that patterns in data can be used to inform solutions to specific problems. Machine learning algorithms employ a variety of pattern recognition and prediction techniques, with one prominent example being the deep neural network (DNN). The DNN has the advantage of being able to recognise patterns in complex and large data sets with greater accuracy by learning the representation of data in each layer of the model [4], [5], [6].

The application of deep neural network technology for the detection of brain tumours in humans represents one of the most prominent instances of machine learning in the health sector, having witnessed significant advancement in recent years [7], [8], [9], [10]. The integration of technology in the health sector, particularly in the context of tumour detection, necessitates a comprehensive understanding of the disease, encompassing its distinctive features and characteristics [11].

Vol. 6, No. 5, October 2025, Page. 3002-3017
https://jutif.if.unsoed.ac.id
DOI: https://doi.org/10.52436/1.jutif.2025.6.5.5106

Brain tumours can be categorised into primary and secondary brain tumours based on their source of spread. Primary brain tumours are defined as brain cell abnormalities that originate from the brain cells themselves, while secondary brain tumours originate from other body cells [12]. The detection of brain tumours typically necessitates the utilisation of techniques such as sampling or biopsy, coupled with the imaging of the interior of the brain through the utilisation of magnetic resonance imaging (MRI) [13]. The biopsy approach exhibits a superior accuracy rate, albeit with a longer processing time than that of MRI imaging. Nevertheless, MRI imaging is indispensable for the delineation of the tumour's location and its dissemination in intricate detail, enabling the differentiation between the soft and hard tissues of the brain [14].

The magnetic resonance imaging (MRI) technique allows for the production of three-dimensional images, which can be classified according to their contrast and luminance characteristics. These include T1-weighted, T1-weighted contrast, T2-weighted and FLAIR imaging. The contrast and luminance of these images can be used to identify specific features of the tumour, such as necrosis, oedema, non-enhancing tumours and enhancing tumours [15].

The semi-automatic or automatic segmentation of brain tumours is currently regarded as a valuable aid to the efficient diagnosis of such lesions. However, the rapid growth of tumour cells represents a significant challenge to the accurate segmentation of these structures. Consequently, there is a clear need for the development of a method or technique capable of accurately segmenting tumours, thus facilitating the distinction between necrosis, oedema, non-enhancing tumours and enhancing tumours [16].

A Convolutional Neural Network (CNN) is a type of deep neural network layer that allows for pattern recognition in the context of image recognition [17]. It is one of the techniques that may be employed in the process of segmenting brain tumours. There are CNN architectures that have the ability to segment both two-dimensional (2D) and three-dimensional (3D) images. Two notable examples are the 2D UNet and the 3D Unet [18].

The 3D UNet architecture effectively utilises spatial information in volumetric data, enhancing segmentation precision by integrating comprehensive spatial context [19]. The objective of this research is to evaluate the efficacy of the 3D UNet architecture in the segmentation of brain tumours, utilising 3D MRI images as the input data, which are instrumental in the diagnosis of brain tumours by medical professionals.

The existing body of research in this field has concentrated on the detection and segmentation of brain tumours, with a variety of methods and algorithms employed in the process. The field of research on brain tumour segmentation and detection using machine learning techniques is expanding, with a growing body of conducted studies. The majority of research in this field is focused on two key areas: data pre-processing to extract meaningful features and the combination of model architectures to achieve high performance in brain tumour segmentation. In this research, the dataset used is BRATS 2021, which consists of 675 datasets with four MRI imaging modes (FLAIR, T1-Weighted, T1-Contrast, and T2-Weighted) and four classes of segmentation labels, namely background, edema, non-enhancing tumour, and enhancing tumour. BRATS 2021 denotes the brain tumour segmentation challenge of 2021, offering datasets for researchers to enhance segmentation algorithms using authentic data [20]. The following recent research studies are of particular note:

This research employs a deep learning method utilising a pre-trained Xception model as its architectural foundation for the classification of brain tumours, namely pituitary, glioma and meningioma. The dataset comprises 4,480 images, of which 2,760 depict diagnosed brain tumours and 1,720 are of healthy tissue. Upon testing the model using the F1-Score metric, the resulting accuracy value was 98.75% [21].

This research employs three stages, namely a high-pass filter, a median filter and a DWAE model, for the detection of brain tumours in magnetic resonance images (MRIs) using five datasets of MRIs of the

Vol. 6, No. 5, October 2025, Page. 3002-3017
https://jutif.if.unsoed.ac.id
DOI: https://doi.org/10.52436/1.jutif.2025.6.5.5106

brain containing images of the five types of brain tumour. The results of the model testing reached an average accuracy value of 99.3% across the BRATS 2012, BRATS 2013, BRATS 2014, 2015 challenge and BRATS 2015 and ISLES datasets. The method developed in this study demonstrates the capacity to analyse a substantial number of images with remarkable efficacy, thereby ensuring the model's remarkable generalisation capabilities [22].

In this study, the self-organising mapping (SOM), K-mean and fuzzy C-mean (FCM) methods were employed to segment regions within the brain tumours. The dataset employed comprises 285 datasets, with the primary focus of this research being region extraction, feature selection, and hybrid segmentation. This approach yields a Dice overlap index value of 0.99 and a Jaccard index of 0.94. The pre-processing with SOFM has a significant impact on the segmentation results produced by the model [23].

This study employed an edge detection algorithm to obtain images of brain tumours from multimodal MRI inputs, resulting in robust edge mapping for tumour identification. The results achieved utilising the proposed method demonstrate high accuracy (0.99) and have the potential to be further developed when combined with other image analysis methods [24]. The application of the YOLOv3 Deep Network to the detection of brain tumours on a portable electromagnetic imaging system yielded enhanced model performance outcomes, utilising the Deep Neural Network (DNN) on extensive training data sets comprising 800 MRI images. The model demonstrated the capacity to process images of dimensions 416 x 416 pixels, attaining an accuracy of 0.95 and a loss of 0.092 [25].

The application of image segmentation in the field of medical imaging is of paramount importance and is experiencing a period of significant growth. Image segmentation is a methodical approach to extracting pertinent information in medical imaging, facilitating the diagnosis of diseases such as tumours and the localisation of tumours [16], [26], [27], [28]. Conversely, the advancement of tumour segmentation is a significant challenge due to the necessity for the development of appropriate algorithms and methodologies to ensure accurate segmentation. Furthermore, the input images, in the form of MRI, encompass a multitude of modalities that are inherently complex and diverse, thereby increasing the complexity of the segmentation process itself. The utilisation of data pre-processing and sophisticated modelling algorithms necessitates a substantial allocation of resources, while the demand for transparency in the processing pipeline to guarantee the acceptability of the output presents an additional challenge.

2. METHOD

2.1. Research Flow

The research stages comprise four principal phases as shown in Figure 1: data acquisition, exploratory data analysis, data pre-processing, model training and model evaluation. The objective of these stages is to ensure the effectiveness of the research process [29].

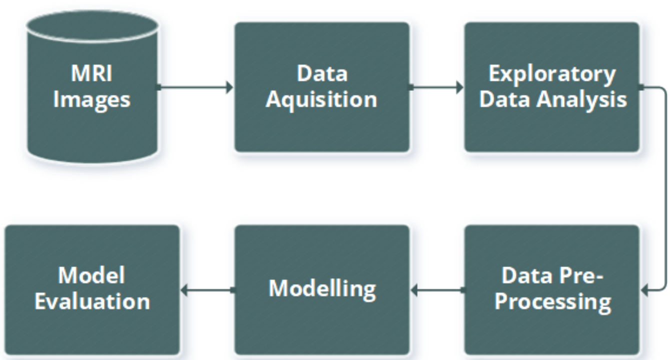

Figure 1. Research flow

Jurnal Teknik Informatika (JUTIF) Vol. 6, No. 5, October 2025, Page. 3002-3017
P-ISSN: 2723-3863 https://jutif.if.unsoed.ac.id
E-ISSN: 2723-3871 DOI: https://doi.org/10.52436/1.jutif.2025.6.5.5106

2.2. Data Acquisition

The dataset was derived from the BRATS (Brain Tumour Segmentation) challenge 2021, which was organised by the Radiological Society of North America (RSNA), the American Society of Neuroradiology (ASNR), and the Medical Image Computing and Computer Assisted Interventions (MICCAI) Society. A total of 675 MRI data sets in neuro-imaging format (Nibabel) were collected, each comprising four files: flair, t1, t1-ce, and t2, as well as seg. The latter is a segmentation class that has been mapped by the data source provider and will serve as the label in the model training process. The remaining files represent the imaging modalities of the magnetic resonance imaging (MRI) machine scans [30].

Table 1. Class segmentation label

Class	Label
0	background
1	edema
2	non-enhancing tumour / necrotic tumor core
3	enhancing tumour

The dataset comprises four MRI modalities: native (T1), T2-weighted (T2), post-contrast T1-weighted (T1ce), and fluid-attenuated inversion recovery (FLAIR). Each modality contains 155 cuts per volume. The data includes labels for three types of brain tumours: enhancing tumour, necrotic, edematous and non-enhancing tumour. Class labels for each brain tumour type are represented in Table 1.

FLAIR is an MRI technique that suppresses cerebrospinal fluid (CSF) signals, thereby facilitating enhanced visualisation of lesions in proximity to the brain ventricles. T1 imaging provides optimal contrast between brain tissue and highlights fat, whereas T1-ce, utilising gadolinium contrast, enhances areas exhibiting increased vascularity or blood-brain barrier breakdown, thereby facilitating the detection of tumours and inflammation. T2 imaging exhibits high contrast between brain tissue and fluid, thus aiding in the detection of oedema and lesions [31]. The Label Segmentation file, containing the results of radiology segmentation and labelling, serves as a reference for brain segmentation prediction. As illustrated in Figure 2, each label in the dataset is presented in a different slice orientation.

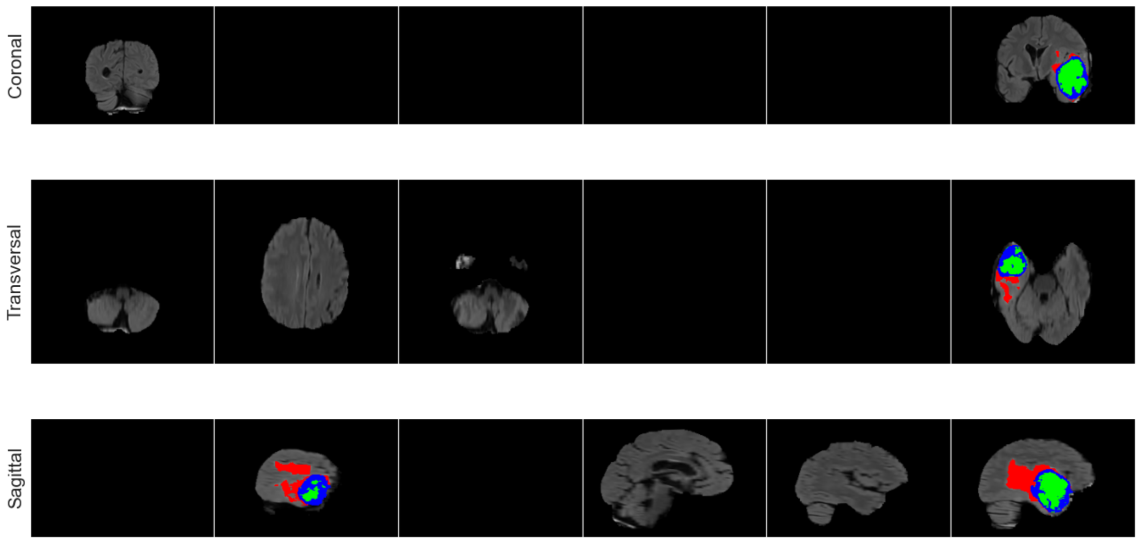

Figure 2. Annotated Brain Magnetic Resonance Imaging Scan, BRATS 2021

Jurnal Teknik Informatika (JUTIF) Vol. 6, No. 5, October 2025, Page. 3002-3017
P-ISSN: 2723-3863 https://jutif.if.unsoed.ac.id
E-ISSN: 2723-3871 DOI: https://doi.org/10.52436/1.jutif.2025.6.5.5106

2.3. Exploratory Data Analysis

The exploratory data analysis stage comprises the process of extracting data features and visualising segmentation images and labels. The objective of this phase is to prepare the pre-processed data in a manner that facilitates efficient, rapid and accurate training of the model, thereby ensuring effective generalisation (good fit) [32].

The visualisation of the four modal image layers with the tumour demonstrated that the FLAIR and T1-Ce imaging had superior visual clarity, with the tumour and other tissue being distinctly delineated (evidencing a clear abnormality) as shown in Figure 3.

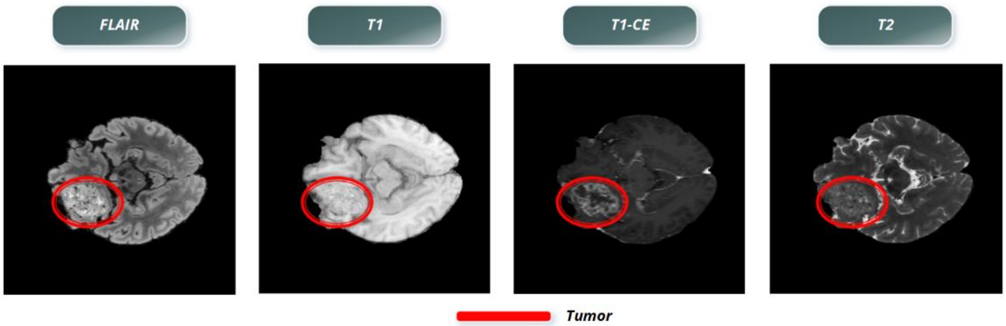

Figure 3. Four-modality MRI imaging of tumours

Additionally, it can be seen in Figure 4 that oedema is the swelling of brain tissue in proximity to a brain tumour, which is caused by the tumour itself rather than by the surrounding non-enhancing tissue.

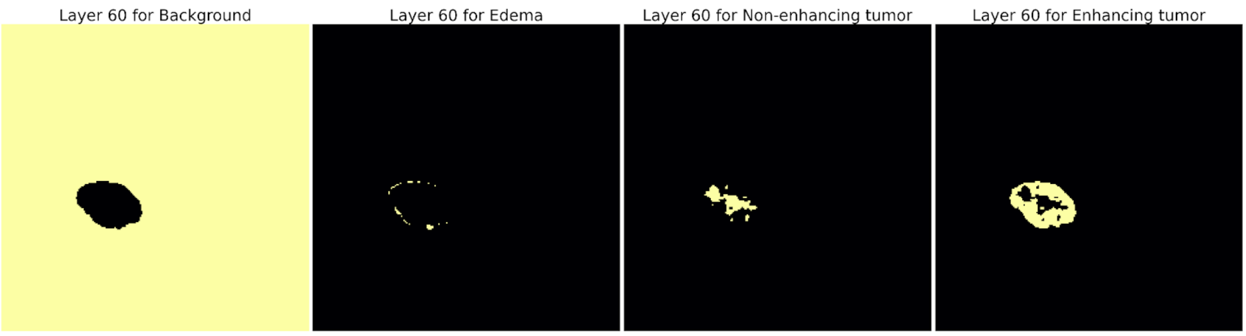

Figure 4. Class label segmentation

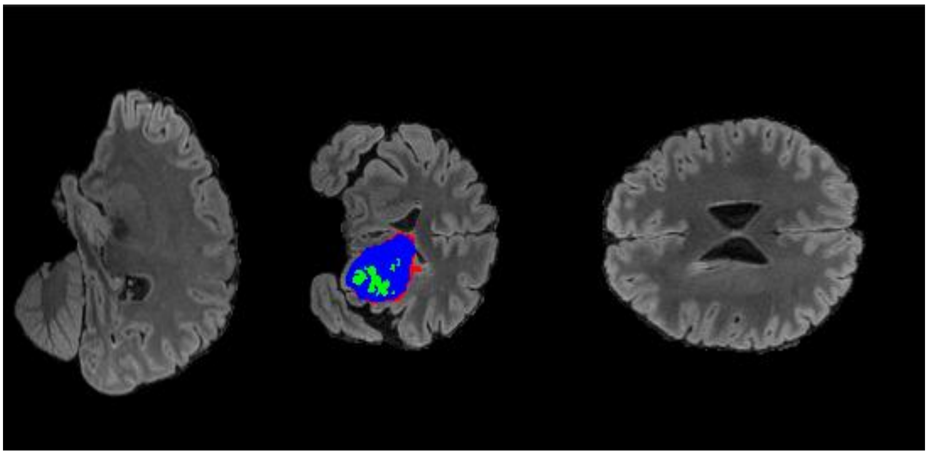

Figure 5. MRI Scan with annotated segmentation label

Jurnal Teknik Informatika (JUTIF) Vol. 6, No. 5, October 2025, Page. 3002-3017
P-ISSN: 2723-3863 https://jutif.if.unsoed.ac.id
E-ISSN: 2723-3871 DOI: https://doi.org/10.52436/1.jutif.2025.6.5.5106

Moreover, when three-dimensional imaging of the MRI scan is conducted in conjunction with the segmentation label, as shown in Figures 5 and 6, a distinct visual representation of the tumour and its precise location is generated. The pixel resolution of the MRI image is (240, 240, 155), with each value representing height, width, and depth, respectively.

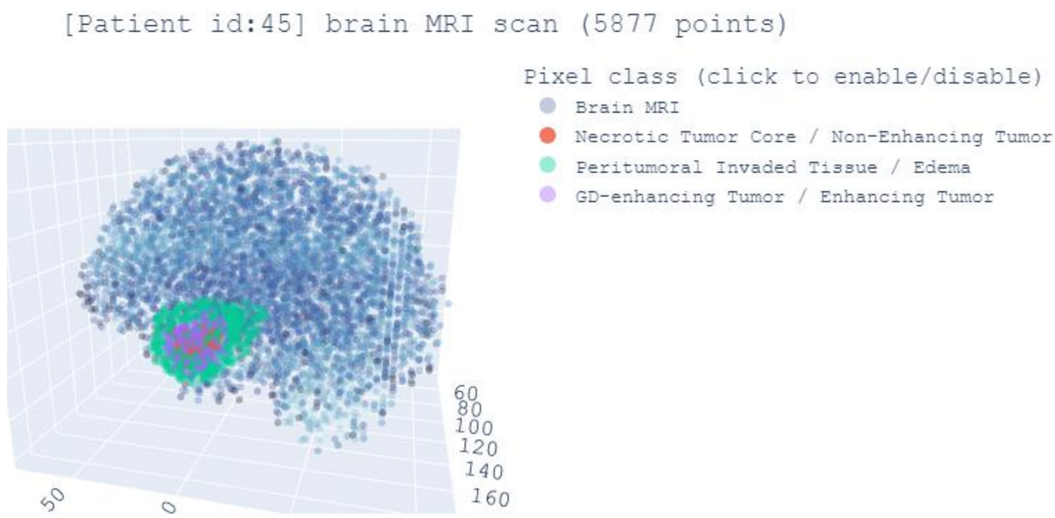

Figure 6. Three-dimensional visualisation MRI Scan with label

The exploratory results of the overall visualisation indicate that the use of diverse MRI imaging modalities can assist the model in differentiating between tumour and general tissue in the brain. Furthermore, the model's processing speed can be enhanced by performing a sub-volume that encompasses solely the tumour area. This approach effectively reduces the input dimension and optimises the training process.

2.4. Data Pre-processing

The input images need to be pre-processed so that they can be efficiently and effectively computed by the model algorithm [33]. The pre-processing steps performed can be seen in Figure 7, which include extracting the image sub-volume containing only the brain tumour area, normalising the pixel value of the image, converting the file to HDF5 format and finally dividing the dataset into several parts, namely the training set and the validation set.

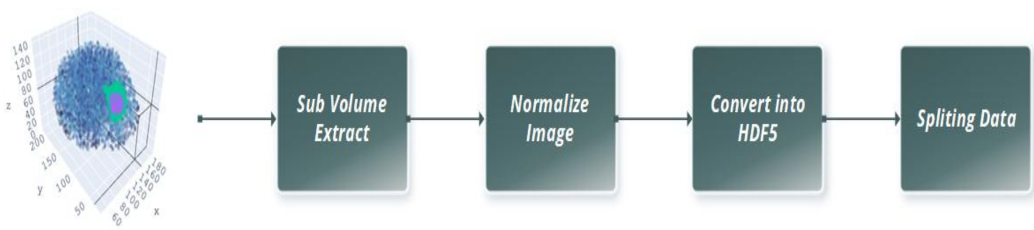

Figure 7. Preprocessing phase

The sub-volume extract changes the dimension from (240, 240, 155) to (160, 160, 16), where the sub-volume obtained is the part of the brain that is the tumour area. The sample of sub-volume and label image is represented in Figure 8.

Vol. 6, No. 5, October 2025, Page. 3002-3017
https://jutif.if.unsoed.ac.id
DOI: https://doi.org/10.52436/1.jutif.2025.6.5.5106

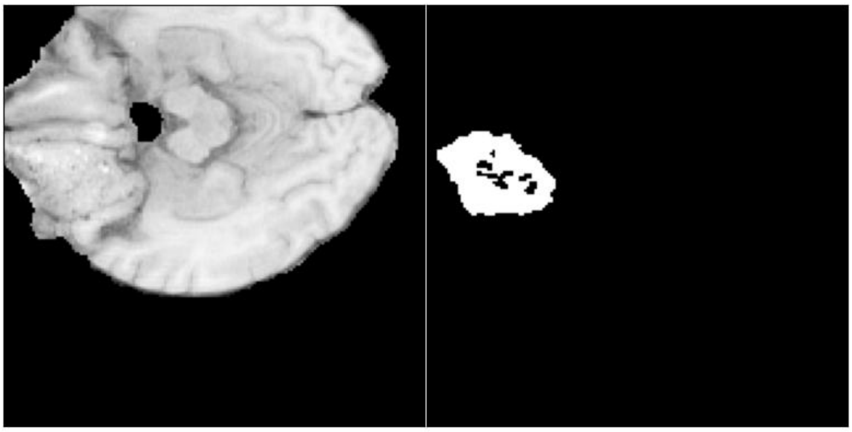

Figure 8. Sub Volume Image and Label

In addition, the sub-volume of the MRI scan is normalised from its pixel value, which previously had a range of 0-255, to 0-1 (1). The normalisation will help to speed up the training process, allowing the model to achieve convergence. The volume is then converted to HDF5 format for storage efficiency and data portability so that it can be processed by the model.

$$X_{scaled} = \frac{X - X_{min}}{X_{max} - X_{min}} \qquad (1)$$

The MRI scan dataset is then divided into two sets, training and validation, with an 8:2 ratio, to evaluate the model's performance against new or unseen data.

2.5. Modeling

The model used in this research is a deep neural network with a convolutional layer, which automatically extracts features before inserting them into the hidden layer to calculate the weighting of the neural network. The convolutional neural network architecture used is a 3D UNet as shown in Figure 9.

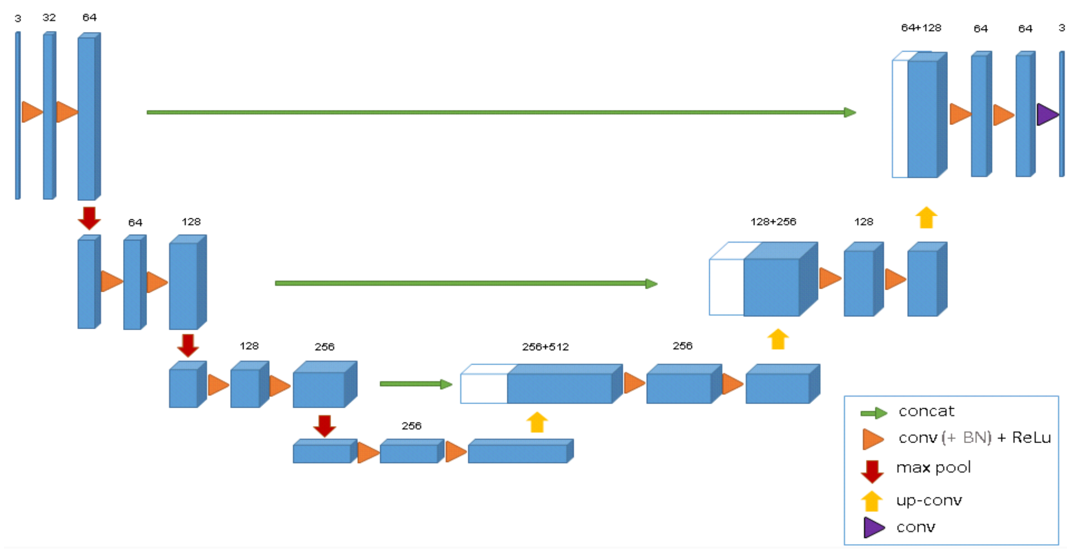

Figure 9. 3D UNet Architecture

Vol. 6, No. 5, October 2025, Page. 3002-3017
https://jutif.if.unsoed.ac.id
DOI: https://doi.org/10.52436/1.jutif.2025.6.5.5106

The 3D UNet architecture has advantages in the task of segmenting large amounts of data. 3D UNet is able to capture the spatial relationship of pixels to the overall volume of the image, making the results more accurate and capable of processing complex images [34].

The layer that plays a role in the feature extraction process is the convolution layer, which functions to multiply the input image with a volume filter to produce a meaningful output or information for the model, and then passes it on to the pooling layer to reduce the image resolution without reducing the information. The process, which can be seen in Figure 10, is repeated continuously.

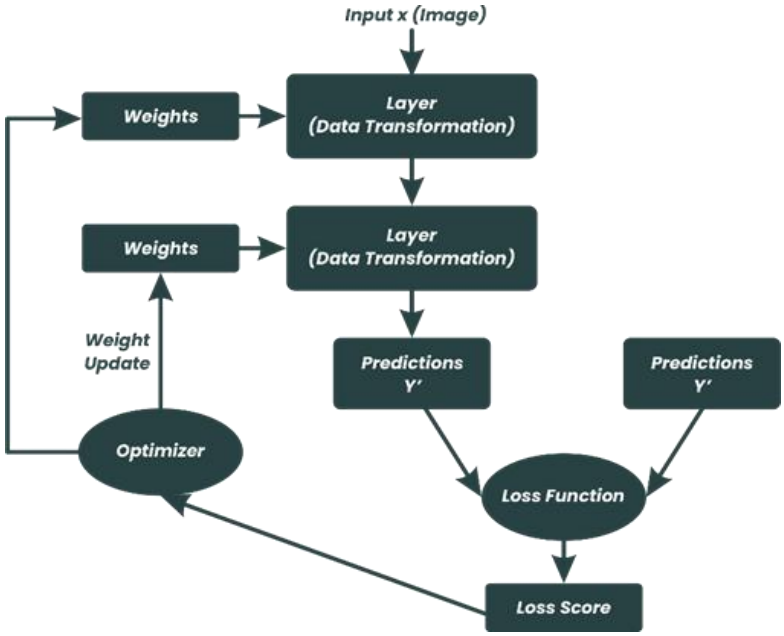

Figure 10. CNN Mechanism

The quality of a Convolutional Neural Network (CNN) is significantly determined by the convolution layer, which serves to extract pixel values from an image by performing multiplication of each m x j pixel with a filter or kernel, which is systematically shifted across the image matrix by n for each i x j pixel (2). The resulting output of the convolution operation is then transmitted to the pooling layer, which serves to reduce the pixel dimension of each image through the application of a max pooling function that identifies and retains the highest pixel value of each i x j pixel.

$$z^1 = h^{1-1} \times W^1 \tag{2}$$

$$ReLU(z_i) = \max(0, z_i) \tag{3}$$

$$h_{xy}^1 = max_{i=0,\ \ j=0}(0, x) \tag{4}$$

The output of the convolution process is first transformed into the ReLU (*Rectified Linear Unit*) activation function (3) before proceeding to the pooling layer (4). The activation function allows CNNs to learn more complex and abstract representations of image data, in addition to ReLU, which helps to prevent vanishing gradients in the model so that the model can be trained more deeply [35].

The convolution layer within the 3D UNet framework incorporates both up-sampling and down-sampling techniques, as illustrated in Figure 11. Up-sampling is employed to rescale pixels to the original dimensions of the input image, while down-sampling is utilized to extract features of reduced dimensionality that retain significant informational content.

Vol. 6, No. 5, October 2025, Page. 3002-3017
https://jutif.if.unsoed.ac.id
DOI: https://doi.org/10.52436/1.jutif.2025.6.5.5106

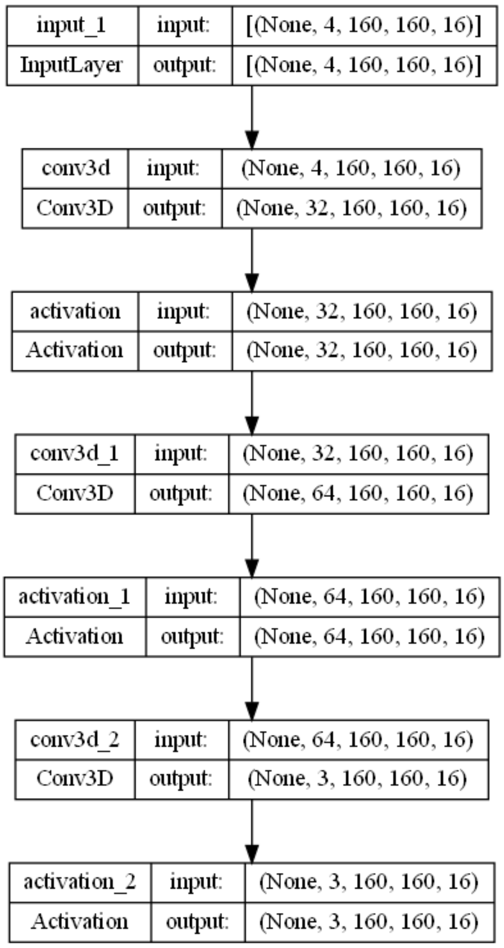

Figure 11. Details layer architecture 3D Unet

The hyperparameters implemented during the training phase include batch size, which denotes the quantity of data processed in a single iteration; epoch, representing the total number of training cycles; learning rate, which indicates the velocity of the machine learning process; and batch normalization, an additional normalization layer applied within UNet to ensure that the values are subsequently appropriate for each layer. The value designated for the hyperparameter represents the upper limit of the computational resource specifications accessible, constrained by the limitations inherent within the research budget, while simultaneously taking into account the ramifications of the research endeavour. The specific values assigned to each hyperparameter are detailed in Table 2.

Table 2. Hyperparameter

No	Hyperparameter	Value
1	Batch Size	2
2	Epoch	50
3	Learning Rate	0.0009
4	Batch Normalization	True

P-ISSN: 2723-3863
https://jutif.if.unsoed.ac.id
E-ISSN: 2723-3871
DOI: https://doi.org/10.52436/1.jutif.2025.6.5.5106

The loss functions used in this model are the soft dice loss (5) and the dice coefficient (6). The cost function is commonly used in segmentation cases with unbalanced data in the training process.

$$\mathcal{L}_{Dice}(p,q) = 1 - \frac{2 \times \sum_{i,j} p_{i,j}\, q_{i,j} + \epsilon}{\left(\sum_{i,j} p_{i,j}^2\right) + \left(\sum_{i,j} q_{i,j}^2\right) + \epsilon} \quad (5)$$

Where,

- p : predictions
- q : the ground truth
- In practice each qi will either be 0 or 1.
- ϵ : small number that is added to avoid division by zero

$$DC(f,x,y) = \frac{1}{C}\sum_{c=1}^{C}\left(DC_c(f,x,y)\right) \quad (6)$$

Where,

- x : the input image
- f(x) : the model output (prediction)
- y : the label (actual ground truth)
- C : number of class category

2.6 Model Evaluation

Model performance assessment is necessary to determine whether the resulting model can effectively and correctly predict the segmentation of brain tumours and has an error value within reasonable limits [36]. The model performance evaluation is based on the confusion matrix provided by the model, which computes the value of accuracy, sensitivity, specificity, false negative rate, false positive rate, precision, and F-1 score metrics for each tumour segmentation class.

$$Recall = \frac{TP}{FN+FN} \quad (7)$$

$$sensitivity = \frac{TP}{TP+TN+FP+FN} \quad (8)$$

$$specificity = \frac{TP}{TP+TN} \quad (9)$$

$$FPR = \frac{FP}{FP+TN} \quad (10)$$

$$FNR = \frac{FN}{FN+TP} \quad (11)$$

$$precision = \frac{TP}{TP+FP} \quad (12)$$

$$F1\ Score = 2 \times \frac{precision \times sensitivity}{precisioin + sensitivity} \quad (13)$$

Where,

- TP : True Positive
- TN : True Negative
- FP : False Positive
- FN : False Negative

Vol. 6, No. 5, October 2025, Page. 3002-3017
https://jutif.if.unsoed.ac.id
DOI: https://doi.org/10.52436/1.jutif.2025.6.5.5106

The term accuracy indicates the ratio of all genuine and non-tumour examples that are accurately categorized, whereas Sensitivity (True Positive Rate) signifies the part of true tumour pixels correctly identified as tumour pixels by the model. The term specificity represents the fraction of true non-tumour pixels that the model successfully categorizes as non-tumour pixels. The FPR (False Positive Rate) and FNR (False Negative Rate) signify the fraction of genuine or non-tumour pixels that are incorrectly categorized as tumour or non-tumour. Precision means the fraction of true tumour pixels that are successfully recognized as tumours and those erroneously designated as tumours. Metrics focusing on precision underscore how well the model performs in pinpointing solely precise tumours among all the predicted tumour pixels [35].

3. RESULT

The model training process was performed on an Intel Core i5 computer platform with 16 GB of RAM and an NVIDIA GTX 1650 accelerator GPU. However, the three-dimensional image training process should require more time and resources to achieve more optimal results.

From Figure 11, it is known that the dimensions of the input and output images are the same size (4, 160, 160, 16) to (3, 160, 160, 16), and the training process is performed up to 50 epochs with the number batch size of 2. The number of batch sizes determines how many images are entered at once in each iteration. Due to platform and resource limitations, the maximum number of batch sizes that can be set is two images.

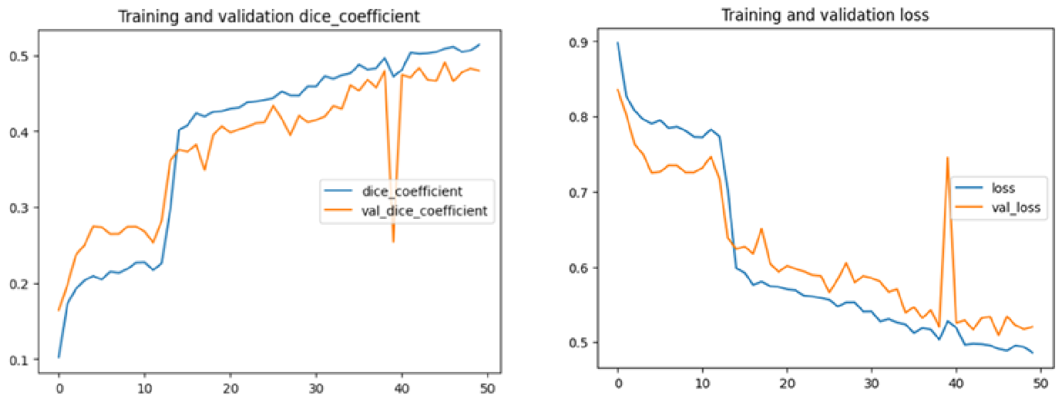

Figure 12. Training and validation each epoch

The graph in Figure 12 shows that the model successfully detects the brain tumour pattern, although the training graph is highly variable. The final training results for the dice coefficient and soft dice loss metrics in the validation are 0.47 (47%) and 0.52 (52%).

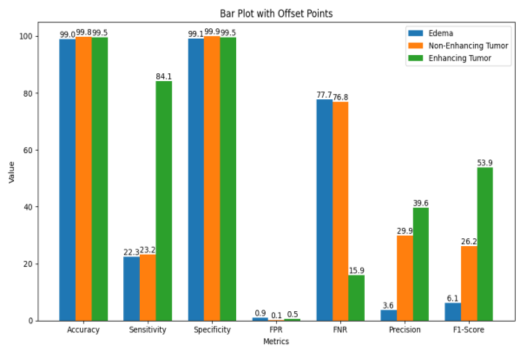

Figure 13. Model evaluation

Jurnal Teknik Informatika (JUTIF)
P-ISSN: 2723-3863
E-ISSN: 2723-3871

Vol. 6, No. 5, October 2025, Page. 3002-3017
https://jutif.if.unsoed.ac.id
DOI: https://doi.org/10.52436/1.jutif.2025.6.5.5106

Based on the evaluation metrics in Figure 13 and Table 3, the model achieved > 99% for the accuracy and specificity metrics. On the contrary, the sensitivity value in this class is only achived at 84.1%.

Table 3. Model performance result

Metric \ Class	Edema Non-Enhancing Tumor	Enhancing Tumor	Non-Enhancing Tumor	Mean
Accuracy	99.0 %	99.5 %	99.8 %	99.43 %
Sensitivity	22.3 %	84.1 %	23.2 %	43.20 %
Specificity	99.1 %	99.5 %	99.9 %	99.50 %
FPR	0.9 %	0.5 %	0.1 %	0.51 %
FNR	77.7 %	15.9 %	76.8 %	56.80 %
Precision	3.6 %	39.6 %	29.9 %	24.37 %
F1-Score	6.1 %	53.9 %	26.2 %	28.73 %

In Figure 14, the model can segment the tumour quite well despite having a low sensitivity metric. This proves that the 3DUNet architecture is able to produce fairly accurate results even with less complex slices.

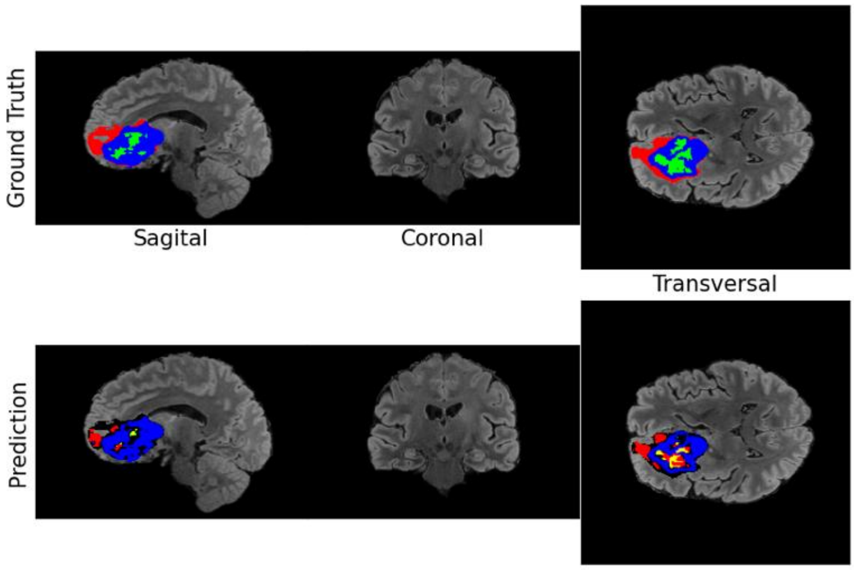

Figure 14. Model segmentation prediction

4. DISCUSSION

This study introduces a Deep Neural Network framework that integrates a soft dice loss function and coefficient as a cost function to improve the segmentation prediction efficacy of the model, particularly in the context of training with imbalanced datasets. This framework employs the 3D UNet architecture, which incorporates a synthesis of convolutional layers and pooling layers typically prevalent in convolutional neural network architectures. The salient distinction of the 3D UNet lies in its dual capability to not only

Vol. 6, No. 5, October 2025, Page. 3002-3017
https://jutif.if.unsoed.ac.id
DOI: https://doi.org/10.52436/1.jutif.2025.6.5.5106

extract relevant information but also to reconstruct the dimensions of critical features to their original scale as a predicted output, specifically the outcome of tumor segmentation.

The implementation of cost function dice coefficients and soft dice loss functions as regulators within the model training paradigm seeks to attain convergence or effective segmentation, particularly in scenarios involving unbalanced label classes, frequently referred to as imbalanced data. Undoubtedly, the situation of imbalanced classes is noticeable in MRI segmentation datasets due to the disproportionate distribution of tumor sections; it is often detected that the edema zone occupies a larger space than the non-enhancing tumor or the opposite.

The performance evaluation metrics encompass accuracy, sensitivity, and specificity. However, in the context of medical applications, the emphasis on model performance predominantly centers on the sensitivity metric, as it is imperative for the model to accurately identify the positive class (tumour) while minimizing the misclassification of other classes. This focus is critical to mitigate the risk associated with misdiagnosing an individual with a tumour as negative. The values attained during the training phase may be regarded as relatively low; nevertheless, when performance is assessed using metrics such as accuracy, sensitivity, specificity, false negative rate, false positive rate, precision, and F-1 score, the model demonstrates commendable performance in certain metrics, particularly accuracy and specificity.

The raised specificity figure highlights the model's superior ability to identify regions free of tumors. In contrast, the sensitivity level is remarkably low, pointing to the model's struggles in effectively delineating tumour zones, aside from the tumour-enhancing sections, which have a sensitivity figure that stands at a relatively high 84.1%. The sensitivity of the model may be significantly improved by integrating supplementary data specifically pertaining to the tumor region or by employing data augmentation strategies such as filtering. Conversely, enhancing the dataset is often more productive than merely using augmentation methods, as it strengthens model generalisation in practical contexts and generates more noticeable progress. This viewpoint is congruent with the overarching transition in machine learning research from a model-centric framework towards a data-centric paradigm.

Table 4. Comparative analysis with previous studies

Research Work	Method	Accuracy	Sensitivity	Specificity
Proposed	3DUNet - CNN	99.43 %	43.2%	99.5 %
Ahmed H [24]	Optimized Edge Detection	99.10%	93.26%	99.98 %
Amran H [25]	YOLOv3 DNN	98.84%	-	-
Isselmou A [22]	DWAE	99.3%	95.6%	96.9%

Table 4 presents a comparative analysis of the performance outcomes associated with the 3DUNet model in conjunction with alternative methodological approaches. The proposed model attains a superior accuracy rate of 99.43% compared to previous studies, alongside a remarkably elevated specificity rate of 99.5%; however, it does not exceed the efficacy levels exhibited by the Optimised Edge Detection technique.

Future research endeavors might focus on the development of more robust model architectures, alongside the integration of the dice loss function and improved preprocessing techniques for the dataset, which could significantly augment model performance in scenarios involving imbalanced datasets.

Vol. 6, No. 5, October 2025, Page. 3002-3017
https://jutif.if.unsoed.ac.id
DOI: https://doi.org/10.52436/1.jutif.2025.6.5.5106

5. CONCLUSION

Brain tumour segmentation is crucial in the process of disease diagnosis and prognosis by doctors. Knowing the spread of the tumour and the areas of the brain affected will help in the pre-surgical process. Through experiments in this research, it is evident that the model with a 3D UNet architecture performs well on complex images, even with limited resources and simple slices. The model achieved high overall accuracy and specificity, with performance levels of 99.43% and 99.5%, respectively, as well as a high sensitivity value in the tumour-enhancing class of 84.1%. By attaining this level of performance, the model can assist medical practitioners in obtaining enhanced insights into the proliferation of tumours and can facilitate more precise treatment planning through segmentation predictions within the surgical environment subsequently. However, limitations in this study, such as the use of limited resources, can be improved in future research. In addition, the performance of the model, especially the sensitivity level, can be further improved by better pre-processing of the dataset or adding more non-enchancing class datasets, so future research is recommended to be data-oriented or data-centric rather than model-centric.

CONFLICT OF INTEREST

The authors declare that there is no conflict of interest between the authors or with research object in this paper.

REFERENCES

[1] M. Li, L. Kuang, S. Xu, and Z. Sha, “Brain Tumor Detection Based on Multimodal Information Fusion and Convolutional Neural Network,” *IEEE Access*, vol. 7, pp. 180134–180146, 2019, doi: 10.1109/ACCESS.2019.2958370.

[2] M. Paluszek and S. Thomas, “An Overview of Machine Learning,” in *MATLAB Machine Learning Recipes*, Berkeley, CA: Apress, 2024, pp. 1–19. doi: 10.1007/978-1-4842-9846-6_1.

[3] A. A. Verma *et al.*, “Implementing machine learning in medicine,” *Canadian Medical Association Journal*, vol. 193, no. 34, pp. E1351–E1357, Aug. 2021, doi: 10.1503/cmaj.202434.

[4] X. Tan *et al.*, “Improving Massive MIMO Message Passing Detectors With Deep Neural Network,” *IEEE Trans. Veh. Technol.*, vol. 69, no. 2, pp. 1267–1280, Feb. 2020, doi: 10.1109/TVT.2019.2960763.

[5] Y.-H. Lee, J. H. Won, S. Kim, Q.-S. Auh, and Y.-K. Noh, “Advantages of deep learning with convolutional neural network in detecting disc displacement of the temporomandibular joint in magnetic resonance imaging,” *Sci Rep*, vol. 12, no. 1, p. 11352, July 2022, doi: 10.1038/s41598-022-15231-5.

[6] A. J. Moshayedi, A. S. Roy, A. Kolahdooz, and Y. Shuxin, “Deep Learning Application Pros And Cons Over Algorithm,” *EAI Endorsed Trans AI Robotics*, vol. 1, pp. 1–13, Feb. 2022, doi: 10.4108/airo.v1i.19.

[7] C. Han *et al.*, “Combining Noise-to-Image and Image-to-Image GANs: Brain MR Image Augmentation for Tumor Detection,” *IEEE Access*, vol. 7, pp. 156966–156977, 2019, doi: 10.1109/ACCESS.2019.2947606.

[8] A. K. Sahoo, P. Parida, K. Muralibabu, and S. Dash, “An improved DNN with FFCM method for multimodal brain tumor segmentation,” *Intelligent Systems with Applications*, vol. 18, p. 200245, May 2023, doi: 10.1016/j.iswa.2023.200245.

[9] Mohammed Ahtesham Farooqui, “Machine Learning in Brain Tumor Diagnosis: Assessing the Efficacy of Diverse Methods,” *pst*, vol. 48, no. 4, pp. 4315–4323, Dec. 2024, doi: 10.52783/pst.1272.

[10] O. Kouli, A. Hassane, D. Badran, T. Kouli, K. Hossain-Ibrahim, and J. D. Steele, “Automated brain tumor identification using magnetic resonance imaging: A systematic review and meta-analysis,” *Neuro-Oncology Advances*, vol. 4, no. 1, p. vdac081, Jan. 2022, doi: 10.1093/noajnl/vdac081.

[11] B. Deepa, M. Murugappan, M. G. Sumithra, M. Mahmud, and M. S. Al-Rakhami, “Pattern Descriptors Orientation and MAP Firefly Algorithm Based Brain Pathology Classification Using

Hybridized Machine Learning Algorithm," *IEEE Access*, vol. 10, pp. 3848–3863, 2022, doi: 10.1109/ACCESS.2021.3100549.

[12] R. Sheard, Ed., *Understanding brain tumours: a guide for people with brain or spinal cord tumours, their families and friends*, May 2022. Woolloomooloo: Cancer Council of New South Wales, 2022.

[13] K. R. Prabha, B. Nataraj, A. Karthikeyan, N. Mukilan, and M. S. Parkavin, "MRI Imaging for the Detection and Diagnosis of Brain Tumors," in *2023 4th International Conference on Smart Electronics and Communication (ICOSEC)*, Trichy, India: IEEE, Sept. 2023, pp. 1541–1546. doi: 10.1109/ICOSEC58147.2023.10276177.

[14] R. Di Bonaventura *et al.*, "Reassessing the Role of Brain Tumor Biopsy in the Era of Advanced Surgical, Molecular, and Imaging Techniques—A Single-Center Experience with Long-Term Follow-Up," *Journal of Personalized Medicine*, vol. 11, no. 9, p. 909, Sept. 2021, doi: 10.3390/jpm11090909.

[15] A. Kirimtat, O. Krejcar, and A. Selamat, "Brain MRI Modality Understanding: A Guide for Image Processing and Segmentation," in *Bioinformatics and Biomedical Engineering*, vol. 12108, I. Rojas, O. Valenzuela, F. Rojas, L. J. Herrera, and F. Ortuño, Eds., Cham: Springer International Publishing, 2020, pp. 705–715. doi: 10.1007/978-3-030-45385-5_63.

[16] A. Pathak, M. Kamani, and R. Priyanka, "Brain Tumor Segmentation Using Modified ResUNET Architecture," in *2023 International Conference on Sustainable Communication Networks and Application (ICSCNA)*, Theni, India: IEEE, Nov. 2023, pp. 1150–1156. doi: 10.1109/ICSCNA58489.2023.10370084.

[17] X. Zhang, X. Zhang, and W. Wang, "Convolutional Neural Network," in *Intelligent Information Processing with Matlab*, Singapore: Springer Nature Singapore, 2023, pp. 39–71. doi: 10.1007/978-981-99-6449-9_2.

[18] D. Gramlich, P. Pauli, C. W. Scherer, F. Allgöwer, and C. Ebenbauer, "Convolutional Neural Networks as 2-D systems." arXiv, 2023. doi: 10.48550/ARXIV.2303.03042.

[19] C.-W. Hsu *et al.*, "Three-dimensional-generator U-net for dual-resonant scanning multiphoton microscopy image inpainting and denoising," *Biomed. Opt. Express*, vol. 13, no. 12, p. 6273, Dec. 2022, doi: 10.1364/BOE.474082.

[20] U. Baid *et al.*, "RSNA-ASNR-MICCAI-BraTS-2021." The Cancer Imaging Archive, 2023. doi: 10.7937/JC8X-9874.

[21] A. Saleh, R. Sukaik, and S. S. Abu-Naser, "Brain Tumor Classification Using Deep Learning," in *2020 International Conference on Assistive and Rehabilitation Technologies (iCareTech)*, Gaza, Palestine: IEEE, Aug. 2020, pp. 131–136. doi: 10.1109/iCareTech49914.2020.00032.

[22] I. Abd El Kader *et al.*, "Brain Tumor Detection and Classification on MR Images by a Deep Wavelet Auto-Encoder Model," *Diagnostics*, vol. 11, no. 9, p. 1589, Aug. 2021, doi: 10.3390/diagnostics11091589.

[23] K. Ejaz, M. S. M. Rahim, U. I. Bajwa, H. Chaudhry, A. Rehman, and F. Ejaz, "Hybrid Segmentation Method With Confidence Region Detection for Tumor Identification," *IEEE Access*, vol. 9, pp. 35256–35278, 2021, doi: 10.1109/ACCESS.2020.3016627.

[24] A. H. Abdel-Gawad, L. A. Said, and A. G. Radwan, "Optimized Edge Detection Technique for Brain Tumor Detection in MR Images," *IEEE Access*, vol. 8, pp. 136243–136259, 2020, doi: 10.1109/ACCESS.2020.3009898.

[25] A. Hossain *et al.*, "A YOLOv3 Deep Neural Network Model to Detect Brain Tumor in Portable Electromagnetic Imaging System," *IEEE Access*, vol. 9, pp. 82647–82660, 2021, doi: 10.1109/ACCESS.2021.3086624.

[26] H. B. Li *et al.*, "The Brain Tumor Segmentation (BraTS) Challenge 2023: Brain MR Image Synthesis for Tumor Segmentation (BraSyn)." arXiv, 2023. doi: 10.48550/ARXIV.2305.09011.

[27] A. S. Reddy and G. Malleswari, "Efficient Brain Tumor Segmentation using Kernel Representation," in *2023 7th International Conference on Intelligent Computing and Control Systems (ICICCS)*, Madurai, India: IEEE, May 2023, pp. 1006–1011. doi: 10.1109/ICICCS56967.2023.10142621.

[28] I. Gammoudi and M. A. Mahjoub, "Brain Tumor Segmentation using Community Detection Algorithm," in *2021 International Conference on Cyberworlds (CW)*, Caen, France: IEEE, Sept. 2021, pp. 57–63. doi: 10.1109/CW52790.2021.00016.

Vol. 6, No. 5, October 2025, Page. 3002-3017
https://jutif.if.unsoed.ac.id
DOI: https://doi.org/10.52436/1.jutif.2025.6.5.5106

[29] A. Géron, *Hands-on machine learning with Scikit-Learn, Keras, and TensorFlow: concepts, tools, and techniques to build intelligent systems*, Second edition. in Covid-19 collection. Beijing Boston Farnham Sebastopol Tokyo: O'Reilly, 2019.
[30] U. Baid *et al.*, "The RSNA-ASNR-MICCAI BraTS 2021 Benchmark on Brain Tumor Segmentation and Radiogenomic Classification," *arXiv.org*. July 2021. Accessed: Aug. 21, 2024. [Online]. Available: https://arxiv.org/abs/2107.02314v2
[31] H. S. Sanjay and M. Niranjanamurthy, *Medical Imaging*, 1st ed. Wiley, 2023. doi: 10.1002/9781119785590.
[32] S. Sandfeld, "Exploratory Data Analysis," in *Materials Data Science*, Cham: Springer International Publishing, 2024, pp. 179–206. doi: 10.1007/978-3-031-46565-9_9.
[33] A. Charpentier, "Pre-processing," in *Insurance, Biases, Discrimination and Fairness*, Cham: Springer Nature Switzerland, 2024, pp. 385–396. doi: 10.1007/978-3-031-49783-4_10.
[34] Ö. Çiçek, A. Abdulkadir, S. S. Lienkamp, T. Brox, and O. Ronneberger, "3D U-Net: Learning Dense Volumetric Segmentation from Sparse Annotation." arXiv, June 2016. Accessed: Sept. 28, 2023. [Online]. Available: http://arxiv.org/abs/1606.06650
[35] I. Goodfellow, Y. Bengio, and A. Courville, *Deep learning*. in Adaptive computation and machine learning. Cambridge, Massachusetts: The MIT Press, 2016.
[36] O. Rainio, J. Teuho, and R. Klén, "Evaluation metrics and statistical tests for machine learning," *Scientific Reports*, vol. 14, no. 1, p. 6086, Mar. 2024, doi: 10.1038/s41598-024-56706-x.